Tapers and tapered couplers were made from this fibre using a butane/oxygen flame as the heat source. Although these tapers routinely exhibited losses of less than 0·1 dB at 1300 nm and 1550 nm, at around 1380 nm the loss was typically 0·4 dB greater, and was sometimes as high as 0·8 dB. The loss spectrum of such a taper is drawn in Fig. 1*b*; a prominent loss peak 0·45 dB high can be seen at 1380 nm, superimposed on a 'background' loss of less than 0·05 dB. The taper had been elongated through 17 mm in about 5 min, an elongation typical for the fabrication of a 50 : 50 coupler.

Similar peaks at 1380 nm appeared in the loss spectra of tapers and couplers elongated using different butane/oxygen flame systems and gas supplies, a hydrogen/oxygen flame system, and even a bunsen burner flame fuelled by 'mains' gas. They also appear in the loss spectra of commercially supplied couplers. The loss peak was also exhibited by fibres which had been heated with the butane/oxygen flame without being elongated—for a 6 mm hot zone, the peak at 1380 nm grew to a steady state value of 0·3 dB above the loss at other wavelengths, within 4 min (well within the time frame of the tapered coupler fabrication).

Water as the source of loss: The coincidence of the peak in the loss spectra of tapers and the familiar water peak of the fibre itself suggests that it is water (in the form of hydroxyl, OH) in the tapers which is causing the loss. This being so, the OH concentration within the tapers is several orders of magnitude greater than that within the untreated fibre, the associated losses being 0·45 dB over ~17 mm and 0·2 dB over 1 km. The loss peak in Fig. 1*b* corresponds to a OH concentration of about 500 ppm in the taper, compared with a concentration of about 0·005 ppm in the untreated fibre.[2,3] Such a large amount of water could not have been present in the core of the fibre prior to heating. It must therefore either have existed before in the outer cladding of the fibre, or have originated from the flame itself, which contains water vapour as a product of the combustion of hydrocarbons (such as butane) or hydrogen with oxygen.

Further tapers were made with the same fibre, but now using one of three available water-free heat sources: an externally flame-heated tubular silica 'oven',[4] an electric arc, and a carbon monoxide/oxygen flame. In none of these tapers did a loss peak appear at 1380 nm; for example, Fig. 1*c* is the loss spectrum of a 17 mm taper produced using the carbon monoxide/oxygen flame. This indicates (*a*) that water is indeed the cause of the loss peak, and (*b*) that this water originates in the flame as a combustion product and then diffuses into the heated fibre.

Practical implications: We have identified the diffusion of water, formed as a combustion product, as a significant loss mechanism in single-mode fibre tapers and taper components. A peak of ~0·4 dB in the spectral loss of the component typically results at wavelengths around 1380 nm, despite the loss being minimal at other wavelengths. This is not a major problem in present single-mode fibre telecommunication lines, which are operated at 1300 nm and 1550 nm partly in order to avoid the water peak of the optical fibre itself.[2,3] Broadband systems may need to utilise WDM channels close to the water peak, and fibre sensors may also need to be operated at such wavelengths. It is even possible that future advances in single-mode fibre fabrication and system design technology will involve operation throughout the wavelength range between 1300 nm and 1550 nm, particularly in short links where the attenuation of the fibre may be insignificant. The elimination of 0·4 dB of loss at 1380 nm in each tapered coupler then becomes very important and, for example, 'wavelength flat' couplers[5] would need to exhibit broadband performance in low-loss as well as in splitting ratio.

This work implies that a water peak should occur in any coupler fabricated using a flame fuelled by a water-producing gas, such as the ever-popular butane, propane or hydrogen, and indeed we have measured it in commercially available couplers. The loss spectra of taper components around 1380 nm are rarely published, although the existence of a water peak may be deduced from some published work.[5]

The water peak can be entirely avoided if a water-free heat source is used in the tapering process. The use of a carbon monoxide/oxygen flame is particularly convenient, despite the obvious toxicity of the fuel, since the same flow control and burner apparatus as used for more conventionally fuelled flames can be utilised. The flame is evidently hot enough to soften silica fibres, and low-loss components can be readily produced. Low-loss tapers without the water peak were also produced with other water-free heat sources (the externally heated silica oven and the electric arc), but use of these requires some modification of the apparatus.

Conclusion: Water vapour given off as a combustion product in a fibre taper elongation system can rapidly diffuse into the heated fibre and cause about 0·4 dB of additional loss, at wavelengths around 1380 nm, in the final taper or coupler. This loss is avoided if a water-free heat source is used to heat the fibres, which can be conveniently achieved by directly replacing the conventional burner fuels (such as butane or hydrogen) with carbon monoxide.

Acknowledgments: We would like to thank Prof. C. D. Hussey for useful discussions. This work was supported by Sumicem Optoelectronics (Ireland) Limited.

T. A. BIRKS
R. P. KENNY
K. P. OAKLEY
C. V. CRYAN

Lightwave Technology Research Centre
University of Limerick
Plassey Technological Park
Limerick, Ireland

28th August 1990

References

1 BRICHENO, T., and FIELDING, A.: 'Stable low-loss single-mode couplers', *Electron. Lett.*, 1984, **20**, pp. 230–232
2 GARRETT, I., and TODD, C. J.: 'Components and systems for long-wavelength monomode fibre transmission', *Optical and Quantum Electronics*, 1982, **14**, pp. 95–143
3 NEUMANN, E.-G.: 'Single-mode fibers' (Springer-Verlag, Berlin, 1988)
4 IMOTO, K., IKUTA, Y., and MAEDA, M.: 'New biconically tapered fibre star coupler: structure and fabrication', *Electron. Lett.*, 1985, **21**, pp. 514–515
5 MORTIMORE, D. B.: 'Wavelength-flattened fused couplers', *Electron. Lett.*, 1985, **21**, pp. 742–743

GRINSCH GaAs/AlGaAs LASER STRUCTURES GROWN BY OMVPE USING A NOVEL ALUMINIUM SOURCE

Indexing term: Semiconductor lasers

GRINSCH GaAs/AlGaAs laser structures grown by OMVPE using a novel aluminium source, trimethylamine alane, have been successfully fabricated. Broad-area lasers made from the material have a threshold current density of 200 A cm^{-2}. A V-grooved laser with a monolithically integrated intracavity loss modulator was used to vary the threshold current from I_{th} = 15 mA at an absorber voltage of V_S = 2·5 V to I_{th} = 210 mA for V_S = −2·5 V.

A disadvantage associated with the growth of AlGaAs by organo-metallic vapour phase epitaxy (OMVPE) is the high carbon content of the layers, typically 10^{16}–10^{18} cm^{-3} depending on growth conditions.[1] This results from the strong aluminium–carbon bond present in the precursor molecule for aluminium, trimethylaluminium (TMAl). An additional concern is the likelihood of the presence of aluminium alkoxides in the TMAl, or triethylaluminium, source because of its high reactivity with oxygen and water.[2] It has been shown that this leads to oxygen incorporation in AlGaAs resulting in

compensation of donors and poor luminescence efficiency by the introduction of deep levels.[3]

A possible alternative aluminium source is trimethylamine alane, $(CH_3)_3N \cdot AlH_3$(TMAAl) which has no direct Al–C bond. This leads to an expectation of lower carbon incorporation and a greatly reduced tendency for reaction with O_2. Abernathy *et al.* have reported the first application to III-V epitaxy by using TMAAl in a metal organic molecular beam epitaxial (MOMBE) growth system.[4] They demonstrated significantly lower oxygen and carbon concentrations in AlGaAs, grown with TMAAl in comparison with commonly used aluminium sources for MOMBE. We report an extension of use of this source to OMVPE and a demonstration of device quality of the material through growth and fabrication of graded index separate confinement heterostructure (GRINSCH) laser structures.

A low pressure OMVPE reactor was used for the growth. The chamber pressure was 30 Torr and the main hydrogen carrier gas flow rate was 6·5 l min^{-1}. It was necessary to use a high gas velocity (> 1 m s^{-1}) in order to minimise predeposition of TMAAl which decomposes at ~100°C.[5] The gallium source was triethylgallium. Arsine was used as the arsenic source. The partial pressure of AsH_3 was varied from 0·20 to 0·45 Torr. Diethylzinc was used as the *p*-type Zn doping source and disilane was utilised for *n*-type Si doping. Most of the laser structures were grown at a substrate temperature of T_G = 700°C.

Strong room temperature photoluminescence was observed for AlGaAs compositions with direct bandgaps. Absence of deep-level emission for energies greater than 0·8 eV (measured using an InGaAs detector) suggests a low level of radiative deep traps caused by oxygen or other defects.[6] Secondary ion mass spectroscopy of AlAs and AlGaAs indicated carbon levels at the detection limits (~2 × 10^{16} cm^{-3}). In contrast to AlGaAs grown with TMAl, AlGaAs grown with TMAAl had very weak carbon-related free-to-bound and donor-to-acceptor transitions in the cathodoluminescence (CL) spectra. CL of the ~120 Å wide quantum well within the GRINSCH structure yielded a peak at 1·535 eV with a full width at half maximum (FWHM) of 6 meV at a temperature of 5·6 K.

The GaAs/AlGaAs GRINSCH laser structure is given in Table 1. Broad-area lasers were fabricated to provide an

Table 1 EPITAXIAL LAYER STRUCTURE OF GRINSCH LASER

Al mole fraction ($Al_xGa_{1-x}As$)	Thickness (nm)	Doping concentration (p, n: cm^{-3})
$x = 0$	200	$p = 1 \times 10^{19}$
$x = 0{\cdot}45 \rightarrow 0$	100	$p = 5 \times 10^{18}$
$x = 0{\cdot}45$	1300	$p = 5 \times 10^{17}$
$x = 0{\cdot}2 \rightarrow 0{\cdot}45$	200	$p = 5 \times 10^{16}$
$x = 0{\cdot}2$	15	—
$x = 0$	12	—
$x = 0{\cdot}2$	15	—
$x = 0{\cdot}45 \rightarrow 0{\cdot}2$	200	$n = 5 \times 10^{16}$
$x = 0 \rightarrow 0{\cdot}45$	100	$n = 3 \times 10^{18}$
$x = 0$	800	$n = 3 \times 10^{18}$

n^+-GaAs substrate

initial indication of material quality as a function of growth parameters. As the growth temperature was increased from T_G = 650°C to 700°C the threshold current density, J_{th}, was reduced by an order of magnitude, i.e., from 2000 A cm^{-2} to 200 A cm^{-2} for cavity lengths, L_C = 1 mm and stripe widths of 80 μm. A decreasing value of J_{th} with increasing T_G has been noted for GaAs/AlGaAs lasers grown by other techniques,[7] and suggests that the optical quality of the AlGaAs improves with higher T_G.

Growth on nonplanar substrates[8] was used to achieve built-in optical and electronic confinement of the active region of the laser structure. A 2 μm thick AlGaAs (x ~ 0·25–0·30) epitaxial layer was first deposited on an n^+ GaAs substrate oriented 2° off (100) towards the nearest (110). The top 1·5 μm of the AlGaAs layer was then made semi-insulating using multiple dose ion implantation of O^+. Si was also implanted to ensure the layer was initially *n*-type. The addition of deep oxygen-related acceptors compensates this layer. Next, V-grooves oriented along the [011] direction were formed using standard photolithographic and etching techniques. Regrowth of the GRINSCH structure (see Table 1) then took place.

Following growth of the structure, devices of length L_C = 500 μm with an intracavity loss modulator[9] were created by applying two photolithographically defined metal contacts to the top layer. The resulting device is shown in Fig. 1. Light power output per facet as a function of pulsed gain current, I_G, for an applied absorber voltage of V_S = 2·5 V is shown in Fig. 2. Laser threshold is approximately I_{th} = 15 mA and the above threshold slope is 0·3 mW mA^{-1} per facet. We have also examined the spectral behaviour of the device with

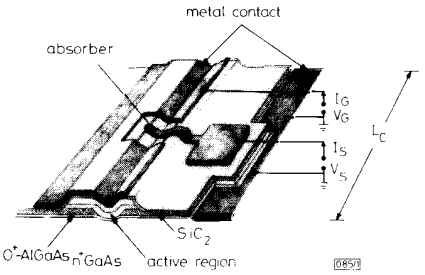

Fig. 1 *GRINSCH single quantum well laser diode*
Grown on V-grooves etched through a 2 μm thick O^+-implanted AlGaAs epitaxial layer

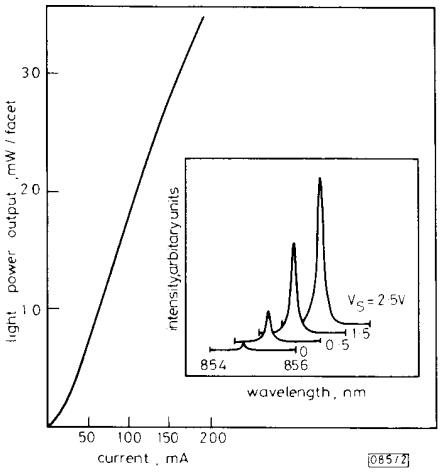

Fig. 2 *Light intensity per facet against pulsed gain current*
V_S = 2·5 V
The inset shows the emission spectra above threshold for several absorber voltages

changing absorber voltage. The inset of Fig. 2 shows the lasing spectrum for applied absorber voltages in the range $0 \leq V_S \leq 2{\cdot}5$ V for a fixed gain section current of I_G = 100 mA. The device lases in a single longitudinal mode and the location of the spectral peak is remarkably insensitive to applied voltage, showing a less than 0·5 Å shift over the entire voltage range. We attribute the absence of a bias controlled wavelength switch between sub-bands in the quantum well[10] to a dominance of cavity losses in the structure over voltage controlled losses. This interpretation is consistent with little variation in the lasing wavelength with voltage controlled losses. Fig. 3 shows the variation of laser threshold, I_{th}, with voltage, V_S, applied to the absorber section. The laser threshold current may be continuously varied through more than an order of magnitude by a 4 V swing of V_S.

In conclusion, we have demonstrated that TMAAl is a promising aluminium precursor in OMVPE and that high

quality AlGaAs layers can be produced. GaAs/AlGaAs V-groove lasers with an efficient intracavity loss modulator have been successfully fabricated using this novel source.

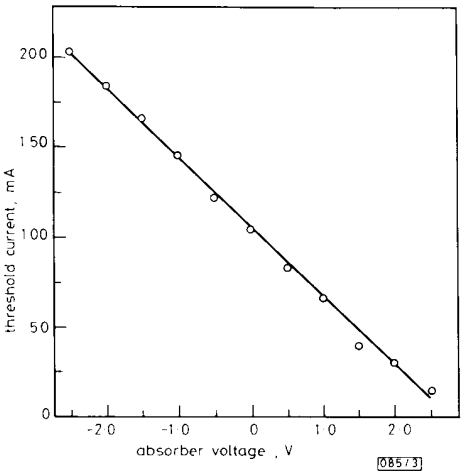

Fig. 3 *Laser threshold current against absorber voltage*

Acknowledgments: We thank R. N. Nottenburg for useful discussions and M. Anzlowar, L. J. Oster, and A. P. Perley for technical assistance.

W. S. HOBSON
A. F. J. LEVI
J. O'GORMAN
S. J. PEARTON
C. R. ABERNATHY
AT&T Bell Laboratories
Murray Hill, New Jersey 07974, USA

V. SWAMINATHAN
AT&T Bell Laboratories
Breinigsville, Pennsylvania 18031, USA

31st August 1990

References

1 KUECH, T. F., WOLFORD, D. J., VEUHOFF, E., DELINE, V., MOONEY, P. M., POTEMSKI, R., and BRADLEY, J.: 'Properties of high purity $Al_xGa_{1-x}As$ grown by the metal-organic vapor-phase-epitaxy technique using methyl precursors', *J. Appl. Phys.*, 1987, **62**, pp. 632–643
2 FRESE, V., REGEL, G. K., HARDTDEGEN, H., BRAUERS, A., BALK, P., HOSTALEK, M., LOKAI, M., POHL, L., MIKLIS, A., and WERNER, K.: 'MOCVD of AlGaAs/GaAs with novel group III compounds', *J. Electronic Mater.*, 1990, **19**, pp. 305–310
3 PEARTON, S. J., IANNUZZI, M. P., REYNOLDS, C. L., and PETICOLAS, L.: 'Formation of thermally stable high-resistivity AlGaAs by oxygen implantation', *Appl. Phys. Lett.*, 1988, **52**, pp. 395–397
4 ABERNATHY, C. R., JORDAN, A. S., PEARTON, S. J., HOBSON, W. S., BOHLING, D. A., and MUHR, G. T.: 'Growth of high quality AlGaAs by metal-organic molecular beam epitaxy using trimethylamine alane', *Appl. Phys. Lett.*, 1990, **56**, pp. 2654–2656
5 RUFF, J. K.: 'Trimethylamine-aluminum hydride and trimethylamine–aluminum chloride dihydride', *Inorg. Synth.*, 1967, **9**, pp. 30–37
6 TSAI, M. J., TASHIMA, M. M., and MOON, R. L.: 'The effects of the growth temperature on $Al_xGa_{1-x}As$ ($0 \leq x \leq 0{\cdot}37$) LED materials grown by OM-VPE', *J. Electronic Mater.*, 1984, **13**, pp. 437–446
7 TSANG, W. T., REINHART, F. K., and DITZENBERGER, J. A.: 'The effect of substrate temperature on the current threshold of GaAs–$Al_xGa_{1-x}As$ double heterostructure lasers grown by molecular beam epitaxy', *Appl. Phys. Lett.*, 1980, **36**, pp. 118–120
8 KAPON, E., YUN, C. P., HARBISON, J. P., FLOREZ, L. T., and STOFFEL, N. G.: 'Low-threshold patterned quantum well lasers grown by molecular beam epitaxy', *Electron. Lett.*, 1988, **24**, pp. 985–986; MARCLAY, E., ARENT, D. J., HARDER, C., MEIER, H. P., WALTER, W., and WEBB, D. J.: 'Scaling of GaAs/AlGaAs laser diodes for submilliampere threshold current', *Electron. Lett.*, 1989, **25**, pp. 892–894
9 LEVI, A. F. J., NOTTENBURG, R. N., NORDIN, R. A., TANBUN-EK, T., and LOGAN, R. A.: 'Multielectrode quantum well laser for digital switching', *Appl. Phys. Lett.*, 1990, **56**, pp. 1095–1097
10 BERTHOLD, K., LEVI, A. F. J., TANBUN-EK, T., and LOGAN, R. A.: 'Wavelength switching in InGaAs/InP quantum well lasers', *Appl. Phys. Lett.*, 1990, **56**, pp. 122–124

SIMPLE DERIVATION OF ADAPTIVE ALGORITHMS FOR ARBITRARY FILTER STRUCTURES

Indexing terms: Adaptive systems and control, Algorithms, Filters

A new method to achieve updating formulas for adaptive filters with arbitrary structures is presented. The well known network sensitivity formula combined with Newton or gradient optimisation schemes gives us the adaptive algorithms. This is illustrated with an adaptive wave digital filter. The derived algorithms use a gradient which is exact in the limit, as the step size tends to zero.

Introduction: The concept of adaptive filter as depicted in Fig. 1 is examined. Our aim is to find the best linear filter, H, so that the estimation error, e, is minimised. To do this we adapt the parameter vector $\hat{\theta}$ at every time instant according to some updating rule.

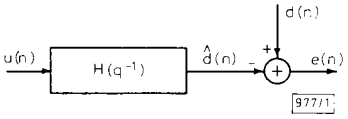

Fig. 1 *Adaptive filter*

Procedures to obtain the updating formulas for adaptive filters implemented with arbitrary structures are presented. The key to the method is the observation that one can obtain the derivative of a transfer function with respect to a network coefficient using the well known network sensitivity formula.[4] One can then use the fact that given the gradient of the error with respect to the parameters it is straightforward to update the parameters in a stochastic gradient or a Newton direction.[3]

The derived algorithms have been used on a number of filter structures and the results are described in detail in Reference 2.

Preliminaries: The Newton and gradient methods which are used to update the adaptive filters are presented. In the following, note that q^{-1} is the backward-shift operator such that $q^{-1}u(n) = u(n-1)$ and that we use column vectors. The aim is to minimise a cost function which, as usual, is chosen as $V(\hat{\theta}) \triangleq E\{\frac{1}{2}e^2\}$. At every time instant, the methods compute an instantaneous estimate of the gradient of $V(\hat{\theta})$ with respect to $\hat{\theta}$ and then updates $\hat{\theta}$ in the approximate negative gradient or Newton direction.[3] Define

$$\psi(n) \triangleq -\text{grad}_{\theta}[e(n)] = \text{grad}_{\theta}[\hat{d}(n)] \tag{1}$$

where both $\hat{\theta}$ and ψ are M-dimensional column vectors.

This leads to the following updating formulas for the Newton algorithm:

$$e(n) = d(n) - \hat{d}(n) \tag{2}$$

$$R(n) = R(n-1) + \gamma(n)[\psi(n)\psi^T(n) - R(n-1)] \tag{3}$$

$$\hat{\theta}(n) = \hat{\theta}(n-1) + \gamma(n)R^{-1}(n)\psi(n)e(n) \tag{4}$$

Here we use a step size $\gamma(n)$ and an approximation of V's Hessian matrix, $R(n) \approx \text{grad}_{\theta}[\text{grad}_{\theta}^T(V)]$.

If we choose a stochastic gradient algorithm instead, $R(n)$ would be replaced with a diagonal matrix containing either a